Journal of Enzyme Inhibition and Medicinal Chemistry

ISSN: 1475-6366 (Print) 1475-6374 (Online) Journal homepage: www.tandfonline.com/journals/ienz20

Evaluation of hydrazone and *N*-acylhydrazone derivatives of vitamin B6 and pyridine-4-carbaldehyde as potential drugs against Alzheimer's disease

Marija Bartolić, Ana Matošević, Nikola Maraković, Valentina Bušić, Sunčica Roca, Dražen Vikić-Topić, Antonio Sabljić, Anita Bosak & Dajana Gašo-Sokač

To cite this article: Marija Bartolić, Ana Matošević, Nikola Maraković, Valentina Bušić, Sunčica Roca, Dražen Vikić-Topić, Antonio Sabljić, Anita Bosak & Dajana Gašo-Sokač (2024) Evaluation of hydrazone and *N*-acylhydrazone derivatives of vitamin B6 and pyridine-4-carbaldehyde as potential drugs against Alzheimer's disease, Journal of Enzyme Inhibition and Medicinal Chemistry, 39:1, 2431832, DOI: 10.1080/14756366.2024.2431832

To link to this article: https://doi.org/10.1080/14756366.2024.2431832

JOURNAL OF ENZYME INHIBITION AND MEDICINAL CHEMISTRY
2024, VOL. 39, NO. 1, 2431832
https://doi.org/10.1080/14756366.2024.2431832

Taylor & Francis
Taylor & Francis Group

RESEARCH ARTICLE

OPEN ACCESS Check for updates

Evaluation of hydrazone and *N*-acylhydrazone derivatives of vitamin B6 and pyridine-4-carbaldehyde as potential drugs against Alzheimer's disease

Marija Bartolić[a], Ana Matošević[a], Nikola Maraković[a], Valentina Bušić[b], Sunčica Roca[c], Dražen Vikić-Topić[c,d], Antonio Sabljić[b], Anita Bosak[a] and Dajana Gašo-Sokač[b]

[a]Division of Toxicology, Institute for Medical Research and Occupational Health, Zagreb, Croatia; [b]Faculty of Food and Technology Osijek, Josip Juraj Strossmayer University of Osijek, Osijek, Croatia; [c]NMR Centre, Rudjer Bošković Institute, Zagreb, Croatia; [d]Department of Natural and Health Sciences, Juraj Dobrila University of Pula, Pula, Croatia

ABSTRACT

The growing prevalence of Alzheimer's disease calls for a drug that can simultaneously act towards several targets involved in the pathophysiology of the disease. In our study, we evaluated the potential of hydrazone and *N*-acylhydrazone derivatives of vitamin B6 and pyridine-4-carbaldehyde to be used as multi-target directed ligands targeting cholinergic system by inhibiting acetyl- and butyrylcholinesterase, lowering the accumulation of β-amyloid plaques by inhibiting both the β-secretase activity and amyloid self-aggregation, and maintaining the biometal balance by chelating certain biometals. Our results showed that all of the tested hydrazones were potent inhibitors of human cholinesterases with inhibition constants (*Ki*) in micromolar range able to lower the activity of β-secretase, inhibit amyloid aggregation, chelate biometals and act as antioxidants. Also, most of them were estimated to be able to cross the blood–brain barrier by passive transport and to be absorbed in human intestines as well as with moderate metabolic stability in liver microsomes.

GRAPHICAL ABSTRACT

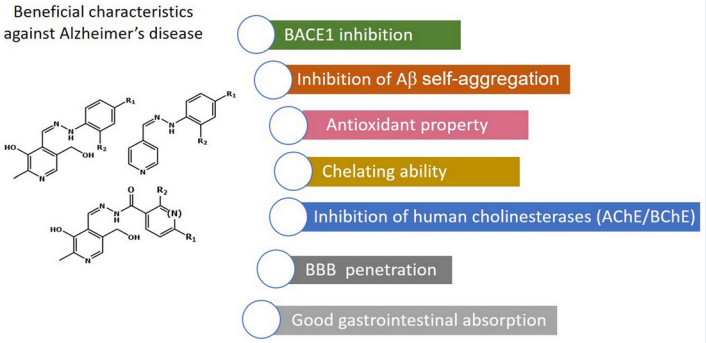

ARTICLE HISTORY
Received 30 July 2024
Revised 8 November 2024
Accepted 14 November 2024

KEYWORDS
N-acylhydrazone; cholinesterase; amyloid self-aggregation; BACE1; chelation

Alzheimer's disease (AD) is a progressive neurodegenerative disease and the most common type of dementia, making up 70% of all dementia cases[1]. It is typically manifested through the progressive loss of short-term memory and cognitive functions accompanied by language and visuospatial skills impairments, motor dysfunctions and changes in personality and behaviour[1,2]. The two major pathological hallmarks of AD are presence of extracellular amyloid plaques and neurofibrillary tangles in the neuronal cytoplasm. Amyloid plaques are a result of accumulation and self-aggregation of amyloid β (Aβ) peptides of various lengths (36–43 amino acids) generated from the amyloid precursor protein (APP) after consecutive proteolytic cleavage by two aspartyl proteases, β-secretase (BACE1) and γ-secretase[3]. Another biochemical feature of AD is the loss of cholinergic neurons, which leads to alterations in acetylcholine neurotransmission and consequently to cognitive dysfunctions[4]. Three out of six FDA-approved and currently used anti-Alzheimer drugs are acetylcholinesterase inhibitors that alleviate symptoms of AD by increasing acetylcholine concentrations in synapses thus enhancing neurotransmission and improving memory deficits[5]. Recently, two monoclonal antibodies have been designed and approved for use in AD[6,7]. The major drawback of all these drugs is that they act only on a single target involved in the mechanism of development or progression of AD, and as such they cannot meet the growing clinical needs. Apart from the major pathological hallmarks, the pathophysiology of AD also includes neuroinflammation[8], biometal dyshomeostasis[9] and overproduction of reactive oxygen species (ROS) that cause oxidative stress[10]. This complex network of various disease-promoting agents calls for the development of more effective drugs by using single molecules that contain more than one pharmacophore

CONTACT Anita Bosak abosak@imi.hr Institute for Medical Research and Occupational Health, Ksaverska Cesta 2, 10000 Zagreb, Croatia; Dajana Gašo-Sokač dajana.gaso@ptfos.hr Faculty of Food Technology Osijek, Josip Juraj Strossmayer University of Osijek, F. Kuhača 18, 31000 Osijek, Croatia.
Supplemental data for this article can be accessed online at https://doi.org/10.1080/14756366.2024.2431832.

capable of modulating different targets relevant for the disease[11]. Following this idea, numerous structural scaffolds and pharmacophores with the potential to affect some of the mechanisms involved in AD development have been used and tested[12–15].

It has been reported that compounds containing a hydrazone functional (=N–NH_2) group show antimicrobial, antibacterial, anti-inflammatory and antitumoral activity[16], as well as antioxidant, anticholinesterase, anti-monoamine oxidase, anti-BACE1 activity and inhibitory activity against fibril formation[16–20]. Moreover, some hydrazone derivatives have shown the potential to act as metal-protein attenuating compounds able to prevent protein aggregation, restore biometal homeostasis and decrease oxidative stress[21,22]. Furthermore, hydrazone derivatives were studied as potential PET (positron emission tomography) imaging agents for amyloid-β plaques[23]. Vitamin B6 represents a group of six compounds (pyridoxine, pyridoxal, pyridoxamine and their phosphorylated forms), all with an important biological role in living organisms acting as a coenzyme in numerous enzyme reactions[24]. Various structurally modified derivatives of vitamin B6 with potential biological activity have been synthesised and tested[25]. Hydrazone derivatives of vitamin B6 have been investigated as potential angiogenesis inhibitors[26] and anti-tuberculosis drugs[27], while the pyridyl-hydrazone derivative of vitamin B6 has been described as a potential antimalarial and antitumor agent[25]. *N*-acylhydrazone moiety has been identified as a very promising motif in drug design and medicinal chemistry due to its presence in compounds acting on many different targets displaying antibacterial, antimycobacterial, antiviral, antitumor, analgesic and anti-inflammatory properties[28,29]. Pyridoxal isonicotinoyl hydrazone (PIH) and its analogues were shown to possess iron-chelating ability, a feature that is very desirable in designing anti-AD drugs, as iron plays a key role in the formation of harmful oxygen radicals and is also involved in a wide range of essential biological functions such as oxygen transport, electron transport and DNA synthesis[30]. As it is estimated that global dementia cases will triple by 2050 due to population growth and ageing, which will undoubtedly present a heavy burden on health systems globally[31], the ongoing search for a drug more effective than the existing ones is very intense. It is desirable that new compounds be synthesized in a safe and energy-efficient way using chemicals whose use assumes a compromise between the economic, social and ecological requirements of the production itself. In line with that, organic synthesis is increasingly oriented towards the development of environmentally friendly processes that use microwave or dielectric heating as an alternative to classical heating[31,32]. The basic advantages of microwave-assisted (MW) synthesis compared to conventional synthesis is the significant shortening of reaction time (from several hours or days to few minutes) and higher reaction yields[33]. Recent studies in the field of green chemistry demonstrated that microwave-assisted synthesis can be used for the preparation of pyridine and vitamin B6 derivatives[34,35], as well as for the synthesis of hydrazone derivatives of vitamin B6, pyridine-4-carbaldehyde and quinoline-2-carbaldehyde in deep eutectic solvents[34].

In this study, we synthesised eight hydrazone derivatives of pyridoxal and pyridine-4-carbaldehyde and eight *N*-acylhydrazone derivatives of pyridoxal and evaluated their biological potential against multiple AD hallmarks: inhibitory potential against acetylcholinesterase (AChE), butyrylcholinesterase (BChE), BACE1 and amyloid self-aggregation, as well as their chelating ability against biometals (Zn(II), Fe(II), Cu (II)), and their antioxidant activity. These groups of compounds were chosen based on the structural similarity of their hydrazone moiety with amidine moiety in BACE1 inhibitors Verbecestat and Atabecestat, compounds which reached phase II clinical trials on AD patients or phase IIb/III clinical trials, respectively, whose high inhibition potency for BACE1 can be ascribed to formation of multiple hydrogen bonds between its amidine moiety and catalytic aspartates of the BACE1 active site[36–39]. The inhibition potency and selectivity of cholinesterases were interpreted and visualised by molecular modelling. Hydrazone derivatives were synthesised using conventional and microwave-assisted synthesis. To additionally explore the possibility of using a more environmentally friendly synthetic route, microwave-assisted synthesis of hydrazone derivatives of pyridoxal and pyridine-4-carbaldehyde was performed in two different solvents, and the yields obtained by all three routes were compared. Since potential drugs for treating neurodegenerative diseases have to reach the brain by penetrating the blood–brain barrier (BBB), we also made *in silico* predictions for a passive crossing of the BBB. Finally, to evaluate the potential of the tested compounds as drugs, the hydrazone derivatives displaying the most potent inhibitory activities were tested for their metabolic stability in human liver microsomes and *in silico* predictions of their human intestinal absorption were estimated.

Materials and methods

Materials

All solvents and reagents for synthesis were purchased and used without further purification: pyridoxal hydrochloride and pyridine-4-carbaldehyde (Aldrich, St. Louis, MO, USA), nicotinohydrazide, isonicotinohydrazide, benzohydrazide, 4-fluorobenzohydrazide, 4-chlorobenzohydrazide, 4-methylbenzohydrazide, 4-nitrobenzohydrazide, 2-hydroxybenzohydrazide, 4-chlorophenylhydrazine hydrochloride, 4-fluorophenylhydrazine hydrochloride (Acros Organics, Antwerp, Belgium), phenyl-hydrazine hydrochloride (Sigma-Aldrich, St. Louis, MO, USA), 2,4-dinitrophenylhydrazine (Merck, Darmstadt, Germany). Fluorescent silica gel plates F254 (Merck, Darmstadt, Germany) and the solvent system chloroform: methanol (4:1) were used for thin-layer chromatography under UV light and wavelengths 254 and 365 nm.

NMR spectra were recorded using a Bruker Avance 300 NMR spectrometer (Bruker BioSpin GmbH, Rheinstetten, Germany) with a 5-mm probe head. The ^{1}H and ^{13}C APT NMR spectra were recorded at 300.130 and 75.468 MHz, respectively. The chemical shifts (δ/ppm) of the ^{1}H and ^{13}C spectra were referenced to the DMSO-d_6 signals (^{1}H: δ = 2.50 ppm; ^{13}C: δ = 39.51 ppm). The assignment of the ^{1}H and ^{13}C signals in the NMR spectra of the compounds was confirmed by cross peaks in the 2D spectra: ^{1}H–^{1}H COSY (Correlation Spectroscopy),^{1}H–^{13}C HMQC (Heteronuclear Multiple Quantum Coherence) and ^{1}H–^{13}C HMBC (Heteronuclear Multiple Bond Correlation). A TFA-d solution was used as an external reference for the ^{19}F spectrum in compound **9** (^{19}F: δ = 11.50 ppm). The ^{19}F NMR spectrum was recorded at 282.231 MHz.

Acetylthiocholine (ATCh) and 5,5′-dithiobis (2-nitrobenzoic acid) (DTNB) were purchased from Sigma-Aldrich, St. Louis, USA. All measurements of cholinesterase activity were done in 0.1 M sodium phosphate buffer (pH 7.4). ATCh and DTNB were dissolved in sodium phosphate buffer. Stock solutions of compounds were prepared in DMSO and all further dilutions were done in water.

Sources of AChE and BChE were recombinant human AChE and purified native human BChE kindly provided by Dr Florian Nachon (Département de Toxicologie, Armed Forces Biomedical Research

Institute, France). The AChE was diluted in a phosphate buffer containing 1% BSA, while further dilutions were made in phosphate buffer with 0.01% BSA. The BChE was diluted in a phosphate buffer containing 0.01% BSA.

For BACE1 activity measurements, a BACE1 Activity Detection Kit was used (Sigma Aldrich, St. Louis, MO, USA). Commercially available β-secretase Inhibitor III (EMD Millipore Corp., Billerica, MA, USA) was used as positive control.

For metal chelation studies, metal salts $ZnCl_2$, $CuCl_2{\cdot}2H_2O$ and $FeCl_2{\cdot}4H_2O$ were used (Sigma Aldrich, St. Louise, SAD).

For amyloid self-aggregation inhibition measurements, HFIP (1,1,1,3,3,3-hexafluoropropan-2-ol) pre-treated human recombinant β Amyloid 1 − 42 (Aβ42) was used as a source of amyloid peptides (Sigma Aldrich, St. Louis, MO, USA). Lyophilised Aβ42 peptides were solubilised in 1% NH_4OH and resuspended in 1× phosphate-buffered saline (PBS) buffer (pH 7.2). Thioflavin T (Sigma Aldrich, St. Louis, MO, USA) was used as a fluorescence dye, while curcumin (Sigma Aldrich, St. Louis, MO, USA) was used as a positive control.

All chemicals for antioxidant activity measurements were purchased from Sigma Aldrich (St. Louis, MO, USA), except for $FeCl_3$ (Kemika, Zagreb, Croatia) and tripyridyltriazine (TPTZ) (Fluka, Buchs, Switzerland). Evaluation of microsomal stability was done by DMPH service at Selvita Ltd., Zagreb, Croatia, using commercially available human liver microsomes (Cat. No. 452117, Corning, USA).

Synthesis

General procedures

To synthesise the target hydrazones (compounds **1–8**), a solution of either pyridoxal hydrochloride or pyridine-4-carbaldehyde (0.74 mmol) was combined with the corresponding phenylhydrazine (1.1 equivalents, 0.81 mmol) in a selected solvent, either ethanol or acetone, following Scheme 1A. The reaction mixture was subjected to heating, either conventionally or using microwave irradiation, until product formation was observed. The resulting crude products were purified by removing residual raw materials and subsequently recrystallised from ethanol. To synthesise *N*-acylhydrazones, we applied the same methodology used for the previously discussed hydrazones. Pyridoxal hydrochloride reacted with either benzohydrazide (yielding compounds **9–14**), nicotine (yielding compound **15**), or isonicotinohydrazide (yielding compound **16**), as illustrated in Scheme 1B.

Conventional synthesis

The solution of pyridoxal hydrochloride or pyridine-4-carbaldehyde and the appropriate phenylhydrazine or *N*-acylhpenylhydrazine in abs. ethanol (10 ml) was mixed on a magnetic stirrer at room temperature for 3 h. The crude product was separated by filtration and purified by washing with cold ethanol and cold diethyl ether and recrystallised from the ethanol to yield products **1**−**16**.

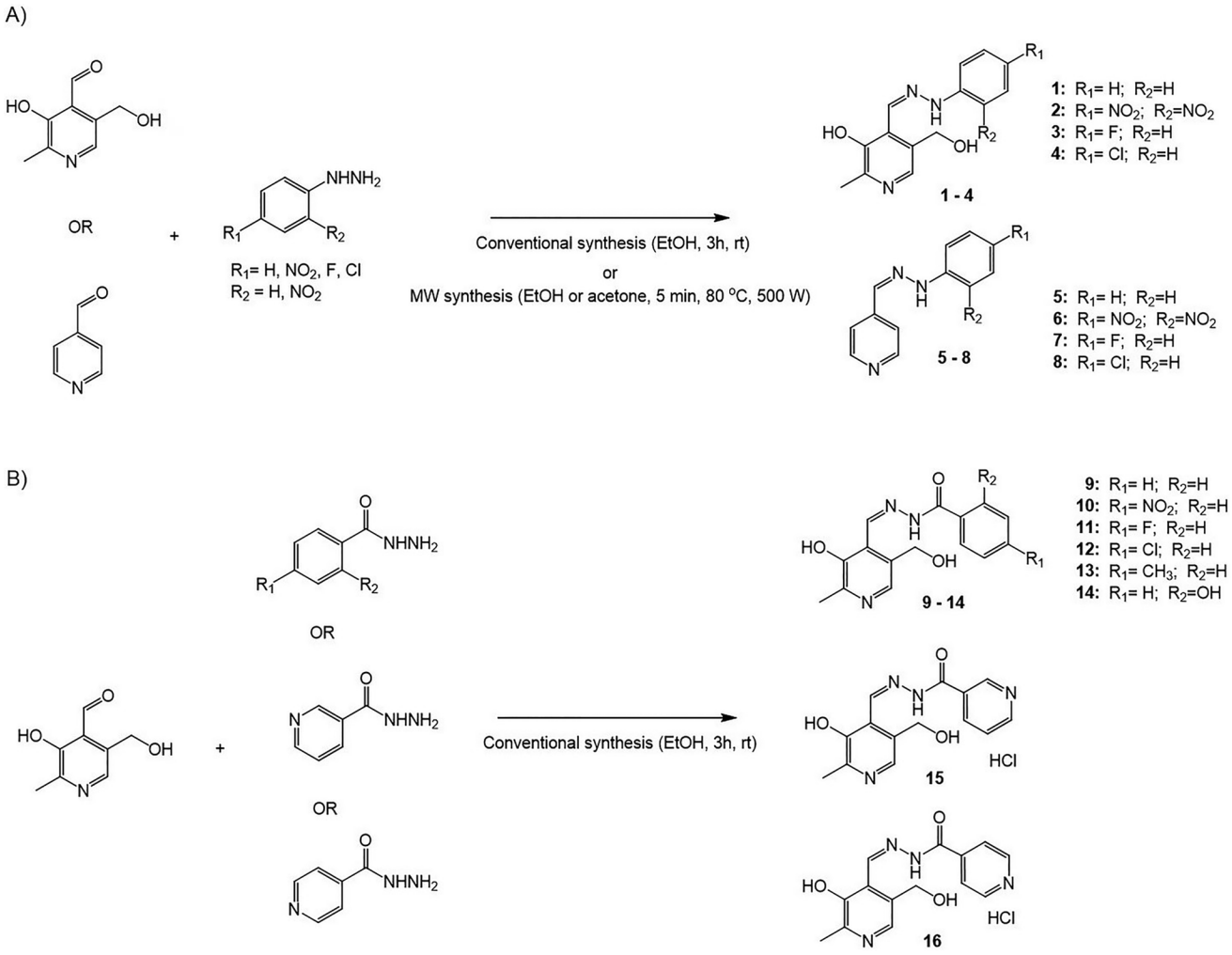

Scheme 1. General procedure for the synthesis of hydrazone derivatives of pyridoxal hydrochloride (**1**−**4**) and pyridine-4-carbaldehyde (**5**–**8**) (panel A) and for the synthesis of *N*-acylhydrazone derivatives of pyridoxal hydrochloride (**9**−**16**) (panel B).

Microwave-assisted synthesis

Microwave-assisted synthesis was performed on a Milestone flexiWAVE (Milestone Srl, Italy). The solution of pyridoxal hydrochloride or pyridine-4-carbaldehyde and the appropriate phenylhydrazine in 10 ml of solvent (ethanol or acetone) was irradiated at 80 °C for 5 min with 500 W. The crude product was separated by filtration and purified by washing with cold ethanol and cold diethyl ether and recrystallised from the ethanol to yield products **1**–**8**.

Biological activity studies

Inhibition of cholinesterase activity

Enzyme activity was measured spectrophotometrically using a slightly modified Ellman method[40], as described earlier[41]. Briefly, AChE and BChE activities were measured at five different ATCh concentrations (up to 0.50 mM in the absence (v_0) and presence (v_i) of different hydrazone concentrations (i; final concentrations of 5 – 300 µM, depending on the compound) needed to obtain 20–80% inhibition of enzyme activity. At least three concentrations of inhibitors for each substrate concentration were used in at least three experiments. To calculate the enzyme-inhibitor dissociation constants (K_i), the Hunter–Downs equation and the linear regression analysis[41] were used:

$$K_{i,app} = \frac{v_i \cdot i}{v_0 - v_i} = K_i + \frac{K_i}{K_S} \cdot s \quad (1)$$

where $K_{i,app}$ stands for the apparent inhibition constant, and K_S for enzyme–substrate dissociation constant. As relatively low substrate concentrations (up to 0.5 mM) were used in the experiments, the equation was used with the assumption that only the substrate binds to the catalytic anionic site (CAS), while the inhibitor can bind to both the CAS and peripheral anionic site (PAS). In the graphical presentation of the Hunter–Dawns equation, the linear dependence of $K_{i,app}$ on the concentration of the substrate shows the competition of the inhibitor with the substrate for binding to the CAS of the enzyme (competitive type; c). In the case of non-competitive binding (n), when the inhibitor binds only to the PAS of the enzyme, $K_{i,app}$ does not depend on the concentration of the substrate. The curve on the Hunter–Downs plot shows mixed inhibition (m) indicating that the inhibitor binds simultaneously to the CAS and PAS.

The final content of DMSO in measurements was up to 3%, and for inhibitory reactions containing more than 0.1% of DMSO and corrected for control reactions containing a corresponding concentration of DMSO. No side interactions of the tested compounds with ATCh or DTNB were detected. Measurements were done at 25 °C on a Tecan Infinite M200Pro (Tecan Austria GmbH, Salzburg, Austria) and SpectraMax iD3 plate reader (Molecular Devices, LLC, San Jose, California, USA) at the wavelength λ = 412 nm. For all calculations, the statistical package GraphPadPrism 8 (Graph Pad Inc, San Diego, USA) was used.

Inhibition of BACE1 activity

Activity of BACE1 was determined using a slightly modified procedure from BACE1 activity Detection Kit[42] as described in a previous work[43]. All hydrazones were dissolved in DMSO (10 mM), and further dilutions were done in FAB (fluorescence assay buffer). The ability of compounds to inhibit BACE1 activity was determined as a percentage from the ratio of fluorescence signals obtained from inhibition reaction (FAB, BACE1, substrate and tested hydrazones with final concentrations of 10 µM and 50 µM, respectively) and control reaction (FAB, BACE1 and substrate only). Non-enzymatic reactions (FAB, substrate and hydrazones) as well as blanks (FAB and substrate only) were also measured and subtracted from inhibition and control reaction, respectively, to eliminate the potential influence of tested hydrazones alone and/or FAB on the intensity of the fluorescence signal. β-secretase Inhibitor III (EMD Millipore Corp., Billerica, MA, USA) (5 µM), used as a positive control, inhibited up to 90% of BACE1 activity, which is in accordance with the manufacturer's data[44]. After the initiation of the enzymatic reaction by addition of BACE1, fluorescence signal readouts were taken at room temperature (25 °C) at zero and two hours after incubation at 37 °C. All readouts were taken with a plate reader (Infinite M200PRO, Tecan Austria GmbH, Salzburg, Austria and SpectraMax iD3, Molecular Devices, LLC, San Jose, CA, USA) with excitation set to 320 nm and emission at 405 nm.

Inhibition of amyloid (Aβ42) self-aggregation

The ability of hydrazones to inhibit the self-aggregation of Aβ42 peptides was measured using the Thioflavin T assay, based on monitoring the change in the fluorescence intensity of Thioflavin T (ThT)[45]. In the presence of compounds that have the ability to interfere with Aβ42 self-aggregation, a decrease in ThT fluorescence occurs[46]. A solution of Aβ42 peptides (final concentration 8 µM) was incubated in the presence (inhibition reaction) and absence (control reaction) of the tested compounds (concentration ratio of Aβ42 peptides and tested compounds in inhibition reaction was 1:1) for 24 h at 37 °C[47,48]. After initial incubation, freshly prepared ThT solution (50 mM glycine–NaOH buffer, pH 8.0) was added (final concentration 20 µM). Reaction mixtures were additionally incubated for 15 min at 25 °C before spectrofluorimetric reading. To determine the potential effect of solvents and compounds on ThT fluorescence, ThT fluorescence was also measured alone with 1× PBS + NH_4OH + DMSO (blank 1) and in the presence of tested compounds and 1× PBS + NH_4OH only (blank 2). All control reactions contained DMSO in concentrations corresponding to the final concentration of the tested compounds. The obtained data was used for background corrections of control and inhibition reactions, respectively. Along with hydrazones, the inhibitory potential of curcumin was also measured as a positive control[49]. Percentage of amyloid self-aggregation inhibition by hydrazones was calculated from a ratio of fluorescence signal of inhibition reaction and of control reaction.

All measurements were performed in 96-well black microplates and readouts were taken with a SpectraMax iD3 plate reader (Molecular Devices, LLC, San Jose, California, USA) with excitation set to 450 nm and emission at 490 nm wavelength.

Metal chelation

The ability of hydrazones to chelate iron, copper and zinc was tested using metal salts $ZnCl_2$, $CuCl_2 \cdot 2H_2O$ and $FeCl_2 \cdot 4H_2O$, according to a previously published protocol[50,51]. Briefly, the absorption spectra of hydrazones (30 µM), metal salt (60 µM), and of the mixture of hydrazones (30 µM) and metal salt (60 µM) were recorded at three time points (1, 30 and 60 min). Changes in the spectra of hydrazone–metal mixture, compared to the spectra of hydrazone and metal alone, indicated the formation of a hydrazone–biometal complex. Additional confirmation of complex formation was done by determining differential UV/VIS spectra as described earlier[50,51]. All spectra recordings and calculations were performed using a UV–Vis spectrophotometer (Cary 300 spectrophotometer Varian, Inc., Australia) as described earlier[50,51].

Antioxidant activity

The antioxidant power of the tested hydrazones was evaluated using the ferric reducing antioxidant power (FRAP) assay according to a slightly modified method by Benzie and Strain[52,53]. The water-soluble derivative of vitamin E (Trolox) and butylated hydroxytoluene (BHT) were used as standard antioxidants. The absorbance was read out at 593 nm using a microplate reader (SpectraMax iD3, Molecular Devices, LLC, San Jose, CA, USA). The reducing capacity was determined for 50 µM hydrazone, the concentration selected according to the value of K_i constants determined for AChE and BChE. All readouts were done against a blank and corrected for the value of absorbance of corresponding hydrazone alone. All measurements were done in three independent experiments. FRAP values were calculated using a standard curve for $Fe_2SO_4{\cdot}7H_2O$.

Docking

For docking ligands into AChE and BChE, crystal structures of recombinant human AChE (PDB ID: 4EY4)[54] and human BChE in the Apo state (PDB ID: 1P0I)[55] were chosen as template structures and typical representatives of the crystal structures of the enzymes in question. The selected PDB structures are optimal since a flexible docking procedure was used where residues freely rotate and numerous different enzyme conformations are generated prior to the docking of compounds. The flexible Docking protocol was used as described earlier[56]. Ligands were minimised and prepared utilising the corresponding protocols implemented in Biovia Discovery Studio Client v21. (Dassault Systèmes, Vélizy-Villacoublay, France). For more details, the reader is referred to SI.

ADME properties

In silico prediction of blood–brain barrier penetration

The potential of all hydrazones to passively cross the blood–brain barrier (BBB) after oral intake was evaluated based on the values of *in silico* determined molecular descriptors: the calculated logarithm of the octanol/water partition coefficient (logP), the molecular weight of hydrazone molecule (MW), the polar surface area (PSA), the number of hydrogen bond donors (HBD), the number of hydrogen bond acceptors (HBA) and the number of rotatable bonds (RB). All data were determined using the Chemicalize 2018 platform[57] and compared to recommended physicochemical properties for successful central nervous system drugs[58].

In silico evaluation of human intestine absorption

The human intestinal absorption prediction was done using the pkCSM online platform[59], which discriminates between intestinally well-absorbed and poorly absorbed molecules. This prediction is based on the lipophilicity of chemicals, evaluated from a partition-coefficient (LogP) value calculated according to the Wildman–Crippen method (WLogP) and their polarity, determined by a calculated topological polar surface area (tPSA) value[59].

Metabolic stability

As a measure of metabolic stability of hydrazones in human liver microsomes, *in vivo* determined hepatic clearance (% LBF) and corresponding clearance classification were used. The source of human microsomes was a commercial product that provides the best representation of an "average patient" fully characterised for many important cytochrome P450, UGTs and other enzymes. According to that classification, compounds with an LBF lower than 30% are classified as compounds with high, 30–70% as moderate and those >70% as compounds with low metabolic stability[60].

In silico evaluation of cytochrome P-450 sub-types inhibition

To additionally elucidate the ability of compounds to affect the drug metabolism through their interaction with cytochrome P450 enzyme superfamily, prediction of compounds' ability to inhibit CYP450 family was estimated *in silico* using online platform pkCSM. Models for different P450 isoforms (CYP1A2, CYP2C19, CYP2C9, CYP2D6 and CYP3A4) were built using data from 18000 compounds whose ability to inhibit CYP P450 has been experimentally determined[61].

Results and discussion

Synthesis

In this paper, four hydrazone derivatives of pyridoxal (**1–4**) and four hydrazone derivatives (**5**–**8**) of pyridine-4-carbaldehyde were prepared (Table 1) by conventional synthesis and MW synthesis in order to determine whether the compounds can be prepared over a shorter time and with higher yields. The yields obtained ranged 11–98%, depending on the compounds and the method used. (Table 1).

Generally, yields for **1**–**4** obtained by both conventional and MW synthesis (in EtOH and acetone) were very close. A slightly higher yield by MW route in EtOH compared to the conventional route and MW synthesis in acetone was observed for **4**. Although the yields were fairly similar, the MW synthesis can be the route of choice because the reaction time was reduced from 3 h for conventional synthesis to only 5 min needed for synthesis using a microwave reactor. Contrary to this, yields for **5**–**8**, the hydrazone derivatives of pyridine-4-carbaldehyde, obtained in acetone using a microwave reactor were much lower (14–24%) compared to conventional synthesis (77–93%). The exception was **6**, with a $-NO_2$ group on the phenylhydrazone moiety, which was obtained in higher yield in the MW synthesis (71% in EtOH and 63% in acetone) compared to conventional synthesis (55%). It was observed that the yields in MW synthesis were lower for all compounds when acetone was used compared to ethanol, which is in accordance with the fact that acetone is a medium microwave absorbing solvent compared to the highly absorbing ethanol. The structures of the **1**–**8** were confirmed on the basis of ^1H and ^{13}C one- and two-dimensional spectra and MS spectra in our previous work[62].

Eight *N*-acylhydrazone derivatives of pyridoxal (**9**–**16**) were successfully prepared by conventional synthesis in high yields ranging from 80 to 98%, therefore an MW-assisted synthetic route was not performed (Table 1). *N*-acylhydrazones (**9**–**16**) were characterised using 1D and 2DNMR spectroscopy. The cross signals obtained by the HMBC NMR technique confirmed the desired structure of the compounds in the DMSO-d_6 solution. All of the recorded spectra, the numbering schemes of the atoms and the tables of chemical shifts, multiplicities and coupling constants are given in Supplementary Information (Scheme S1, Tables S1–S3, and Figures S1–S36).

Inhibition of cholinesterases

Fifteen compounds were tested for their ability to inhibit the action of AChE and BChE. Compound **6** (hydrazone derivative of

Table 1. Yields (%) obtained for the prepared compounds (**1**–**16**) in conventional and microwave-assisted synthesis (MW).

Compound	Conventional synthesis	MW synthesis in EtOH	MW synthesis in acetone
1	78	69	60
2	78	79	63
3	66	73	62
4	74	88	71
5	93	35	24
6	55	71	63
7	77	14	11
8	77	24	14
9	97	–	–
10	90	–	–
11	90	–	–
12	80	–	–
13	95	–	–
14	98	–	–
15	94	–	–
16	95	–	–

Table 2. Reversible inhibition of $hAChE_{rec}$ and hBChE by hydrazones.

Compound	AChE K_i/μM	BChE K_i/μM	$K_{i(AChE)}/K_{i(BChE)}$
1	77 ± 9 (m)	10 ± 2	7.7
2	16 ± 1 (n)	*n.d.*	–
3	59 ± 6 (m)	87 ± 13	0.68
4	38 ± 5 (m)	25 ± 5	1.5
5	301 ± 34 (m)	32 ± 7	9.4
7	211 ± 23 (n)	254 ± 59	0.83
8	155 ± 12 (n)	51 ± 11	3.0
9	199 ± 17 (c)	135 ± 7	1.5
10	131 ± 13 (m)	121 ± 4	1.1
11	126 ± 1 (c)	58 ± 2	2.2
12	89 ± 5 (m)	68 ± 3	1.3
13	102 ± 3 (c)	38 ± 6	2.7
14	192 ± 12 (c)	90 ± 9	2.1
15	120 ± 8 (c)	98 ± 7	1.2
16	144 ± 6 (c)	63 ± 3	2.3
Galantamine[63]	0.52 ± 0.03	1.08 ± 0.08	0.48
Donepezil[63]	0.024 ± 0.007	2.33 ± 0.73	0.010

All data were obtained from at least three experiments.
n.d. not determined; c, n and m stands for competitive, non-competitive and mixed type of inhibition, respectively.

pyridine-4-carbaldehyde and 2,4-dinitrophenylhydrazine) was not tested due to its poor solubility and very fast precipitation in water containing medium. The tested compounds were divided into three groups: the first group consisting of four derivatives of pyridoxal and the second of three pyridine-4-carbaldehyde derivatives, while the third group consisted of eight *N*-acylhydrazone derivatives of pyridoxal.

Generally, all of the tested compounds reversibly inhibited both cholinesterases, AChE and BChE, in micromolar range with inhibition constants (K_i) ranging from 10 to 301 μM (Table 2).

As for AChE, the hydrazones derived from pyridoxal-inhibited AChE, with inhibition constants (K_i) ranging from 16 to 77 μM, were generally more potent inhibitors compared to the hydrazones derived from pyridine-4-carbaldehyde and all of the tested *N*-acylhydrazones which inhibited AChE with a K_i ranging from 155 to 301 μM, and 89 to 199 μM, respectively. The most potent inhibitor was **2**, a hydrazone derivative of pyridoxal and 2,4-dinitrophenylamine, with K_i = 16 μM, which was about 5 times more potent compared to **1**. Compared to Donepezil and Galantamine, drugs used today for the treatment of AD, compound **2** was 670 and 31 times, respectively, a less potent inhibitor of AChE. The difference in inhibition potency between compound **1** and **2** is a result of the different accommodation of the said compounds in the AChE active site which we assessed using molecular docking (Figure 1). Compound **1** was predicted to accommodate in the catalytic site and is well-stabilised by electrostatic interaction with Glu202, an amino acid located next to the catalytic Ser203, and multiple hydrogen bonds and electrostatic π-cation and π-anion interactions with surrounding amino acid residues. On the contrary, **2** partially occupied the catalytic and peripheral site, but achieved a significantly higher number of interactions with PAS (Tables S4 and S5). A list of all of the interactions between the tested compounds **1**–**16** and AChE is displayed in Tables S4–S19.

Among the hydrazones derived from pyridine-4-carbaldehyde, the most potent AChE inhibitor was **8,** with 4-fluorophenylamine. Although each of the two groups were represented by a small number of compounds, a certain trend in inhibition potency could be observed. For both groups of hydrazones, the introduction of a substituent on the phenylhydrazone part of the molecule increased the inhibition power of the molecule compared to its unsubstituted analogues, **1** and **5**.

Additionally, it seems that an increase in the volume of the electron withdrawing group followed the increase in inhibition potency. In the group of *N*-acylhydrazones, a similar effect of the introduction of substituents on the inhibition potential was observed, although more discrete than in the previous two groups of hydrazones. From that group of compounds, the most potent inhibitor was **12**, a 4-chlorohydrazone derivative of pyridoxal, which was twice more potent than its parent **9**. Additionally, the introduction of nicotinic or isonicotinic moiety in the structure of *N*-acylhdrazones, as it is in **15** and **16**, did not have any noticeable effect on their inhibition potency compared to other *N*-acylhydrazones in the group. The inhibition potency of the *N*-acylhydrazones tested here was about two orders of magnitude less potent compared to the hydrazone derivatives of 3-chlorobenzohydrazide[64].

To evaluate the ability of compounds to prevent the formation of the stable AChE-Aß complex through interactions with amino acids from the AChE PAS and form toxic Aß peptide aggregates, compounds which displayed non-competitive or mixed inhibition were singled out (Table 2). Most of the tested compounds inhibited AChE, displaying non-competitive and mixed inhibition without clear connections with their structure. A non-competitive inhibition was displayed by **2**, **7** and **8**, while compounds **1**, **3**–**5**, **10** and **12** exhibited mixed inhibition. In line with that, docking results supported our kinetic results in terms of accommodation of the compounds into the AChE active site gorge and formation of favourable interactions with amino acids from CAS and PAS. However, the purpose of the molecular modelling tools used in this work was to provide an explanation for the observed kinetic differences among the tested compounds by illustrating binding modes and predicting nonbinding interactions of the compounds of interest, for which flexible molecular docking was used. In order to obtain more information about the mechanisms of action of the tested hydrazones and cholinesterases, it is necessary to apply more detailed *in silico* methods, including molecular dynamics simulations or density functional theory calculations[65,66].

Inhibition of BChE was determined for 14 compounds with inhibition constants ranging from 10 to 254 μM, among which compound **1** was the most potent inhibitor of BChE. Compared to Donepezil and Galantamine, **1** was 4 and 9 times less potent in inhibiting BChE, respectively. As inhibition by the highest concentration of **2** used in the assay (100 μM) was lower than 20%, and due to its precipitation in reaction medium, its inhibition constant

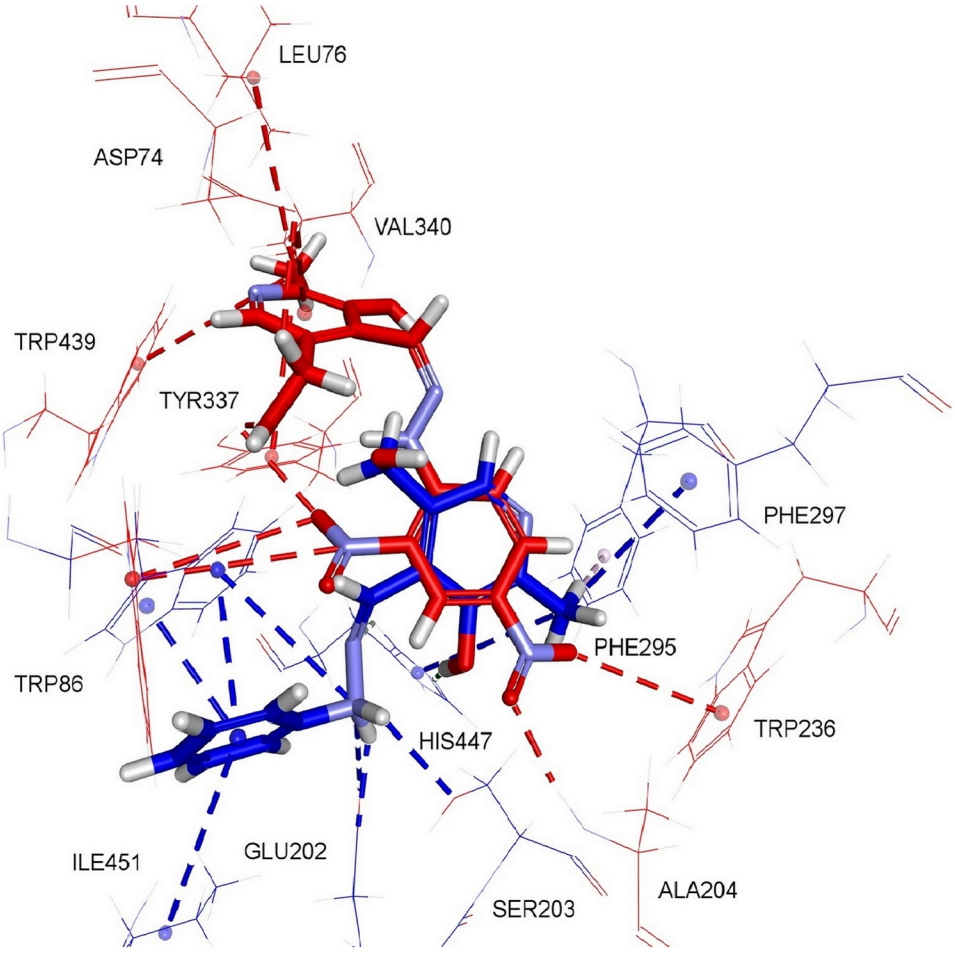

Figure 1. Complex of AChE and **1** (carbon atoms and interactions in blue) and **2** (carbon atoms and interactions in red).

was not determined. Contrary to AChE, no significant difference in inhibition potency between the two groups of hydrazone derivatives was observed. Nevertheless, the results showed that the most potent inhibitors from each group were compounds without a substitution on the phenylhydrazone part of the molecule (**1** and **5**), while compounds with fluorine on the phenylhydrazone part of the molecule (**3** and **7**) were the least potent, suggesting that the addition of electron withdrawing groups can cause a decrease in inhibition potency towards BChE. Compound **1** is predicted to be well stabilised with half a dozen conventional hydrogen bonds with surrounding water molecules and catalytic site amino acids, including both Ser198 and His438 from catalytic triad, compared to **3** which is bound more loosely with a smaller number of interactions, especially in the choline binding site (Figure 2; Tables S20 and S22).

Unlike the hydrazone groups, the inhibition potency of *N*-acylhydrazones increased with the addition of halogen substituents in the benzohydrazyde part of the molecule (**11**–**13**) compared to their unsubstituted analogue, **9**. Moreover, it seems that the inhibition of BChE by *N*-acylhydrazones was affected by the electronegativity of the substituent on the benzohydrazide part of the molecule, as the most potent inhibitor was the compound with an electron donating methyl group (**13**), while the addition of a strongly electron withdrawing—NO_2 group (**10**) did not affect the inhibition potency compared to the unsubstituted **9**. This agrees with an almost twofold increase in the number of non-bonding interactions of *N*-acylhydrazone **13** compared to *N*-acylhydrazones **9** and **10**, with most of the additional interactions being of hydrophobic-(π)-alkyl type and occurring through the methyl-substituted benzohydrazide part of the molecule (Figure 3, Tables S28, S29 and S32). A list of all of the interactions between tested compounds **1**–**16** and BChE is displayed in Tables S20–S35.

It can be noticed that the addition of a hydroxyl group (**14**) or introduction of nicotinic (**15**) or isonicotinic (**16**) moiety in the molecule caused a small, but noticeable increase of inhibition potency compared to **9**.

According to recent studies on the pathophysiology of AD and development of drugs, compounds that are non-selective or even selective to BChE could be more effective in the treatment of middle and final stages of disease, in line with studies which showed that, with the progression of the disease, BChE activity increases, while that of AChE decreases[67]. In our paper, **1** and **5** (both with an unsubstituted phenylamino part of the molecule) were about 8 times more selective to BChE. The rest of the compounds were up to three times more selective to one of the cholinesterases. Interestingly, compounds with fluorine (**3** and **7**) showed only a slight preference towards AChE.

Inhibition of BACE1

As inhibition of BACE1 represents a possible strategy for treatment of Alzheimer's disease, we tested the ability of compounds to

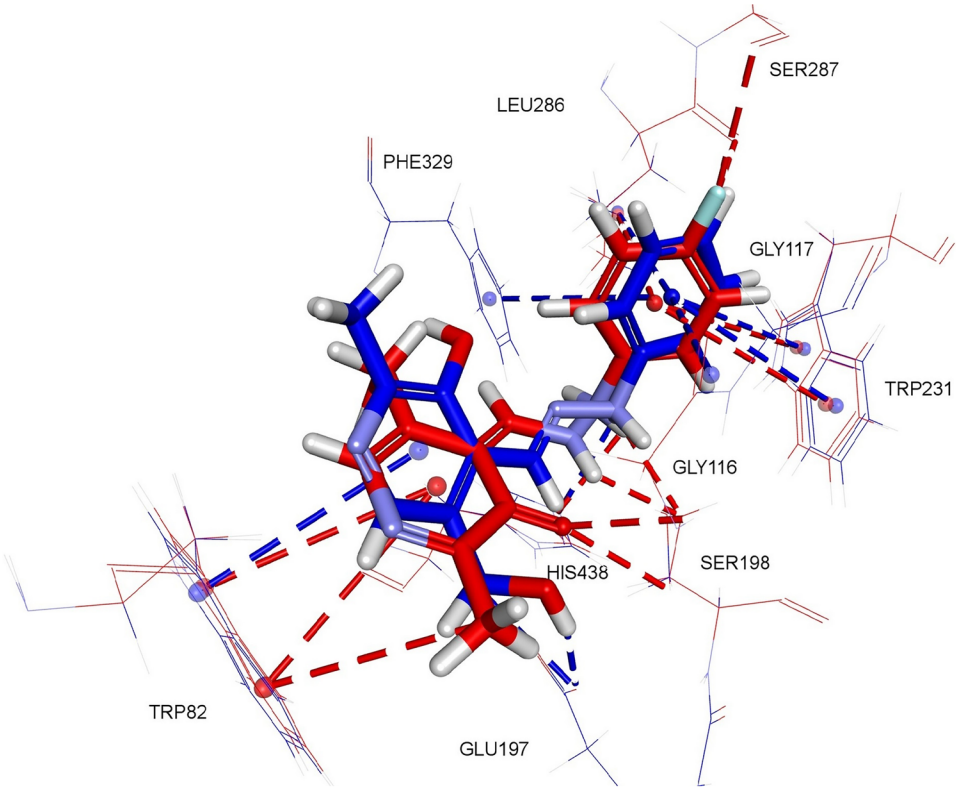

Figure 2. Complex of BChE and **1** (carbon atoms and interactions in blue) and **3** (carbon atoms and interactions in red).

inhibit its action. As a measure of inhibition potency, the percentage of inhibition of BACE1 by 10 and 50 µM of compounds was used (Figure 4). Concentrations were selected based on results of cholinesterase inhibition and corresponded to the determined K_i constants, also keeping in mind the solubility of the compounds.

Our results showed that all of the tested compounds inhibited activity of BACE1 at both concentrations by 10–69%. Only compounds **15** and **16** inhibited BACE1 less than 10% at 10 µM. Although some of these percentages are high, from the viewpoint of developing drugs for the central nervous system, what interests us the most are compounds that inhibit BACE1 activity by less than 50%. This is because studies on BACE1 involvement in Alzheimer's disease and results of clinical trials on drugs targeting primarily BACE1, showed that inhibition lower than 50%, as is the case for naturally occurring Icelandic APP mutation, can provide protection against AD without unwanted side effects in the nervous system[36,68,69]. Percentages of inhibition by 10 µM compounds meet that criterion, as do most of the compounds at 50 µM. The only exception was **2**, a derivative of pyridoxal and 2,4-dinitrophenylhydrazine, which inhibited BACE1 by 69% at the 50 µM concentration and could therefore be expected to cause side effects related to BACE1inhibition.

Inhibition of amyloid self-aggregation

All hydrazones, except for compound **6**, were tested to evaluate their potential to inhibit self-aggregation of Aβ42 peptides. All 15 compounds inhibited aggregation of Aβ42 peptides by 11–37% (Figure 5). The most potent inhibitors were *N*-acylhydrazones **10**, **12** and **14**, which inhibited amyloid aggregation about 36%, followed by **3** and **11** with about 30% of inhibition of amyloid self-aggregation. Those compounds were about 1.5 less potent than curcumin, which was used as a positive control. Less than 10% of inhibition was seen only in **7**. The inhibition percentages of the tested hydrazones are comparable with the IC_{50} values obtained for 1,4-substituted 4-(1H)-pyridylene-hydrazone-type of inhibitors of fibril building[20], pointing to the importance of hydrazine moiety in inhibition of amyloid-β aggregation or fibril destruction.

In vitro antioxidant potential of hydrazones

The reducing capacity of newly-synthesised hydrazone derivatives was expressed as FRAP value, as presented in Figure 6. Generally, all compounds were very good reductants comparable to that of standard antioxidants Trolox and BHT. Most of the compounds showed better or similar reducing ability to that of BHT, while 7 compounds (**1**, **3**, **4**, **5**, **7**, **8**, **10**) showed better reducing ability compared to Trolox. Hydrazone derivatives of pyridoxal and pyridine-4-carbaldehyde were generally very potent antioxidants, of which compounds **1**, **3** and **4** were two times more potent than Trolox. The only exception was compound **2** with an NO_2-substitued phenylhydrazone group, which was less potent than Trolox. When it comes to *N*-acylhydrazone derivatives, only compound **10** had a greater reducing ability compared to Trolox and BHT.

Metal chelation study

The ability of all of the hydrazones to chelate biometal ions Fe^{2+}, Zn^{2+} and Cu^{2+} was tested. Only compound **6** was not tested due to its poor solubility in assay conditions. The absorbance spectra of hydrazones and biometals mixture were recorded at 1, 30 and 60 min after mixing. The spectra recorded after a 30 min

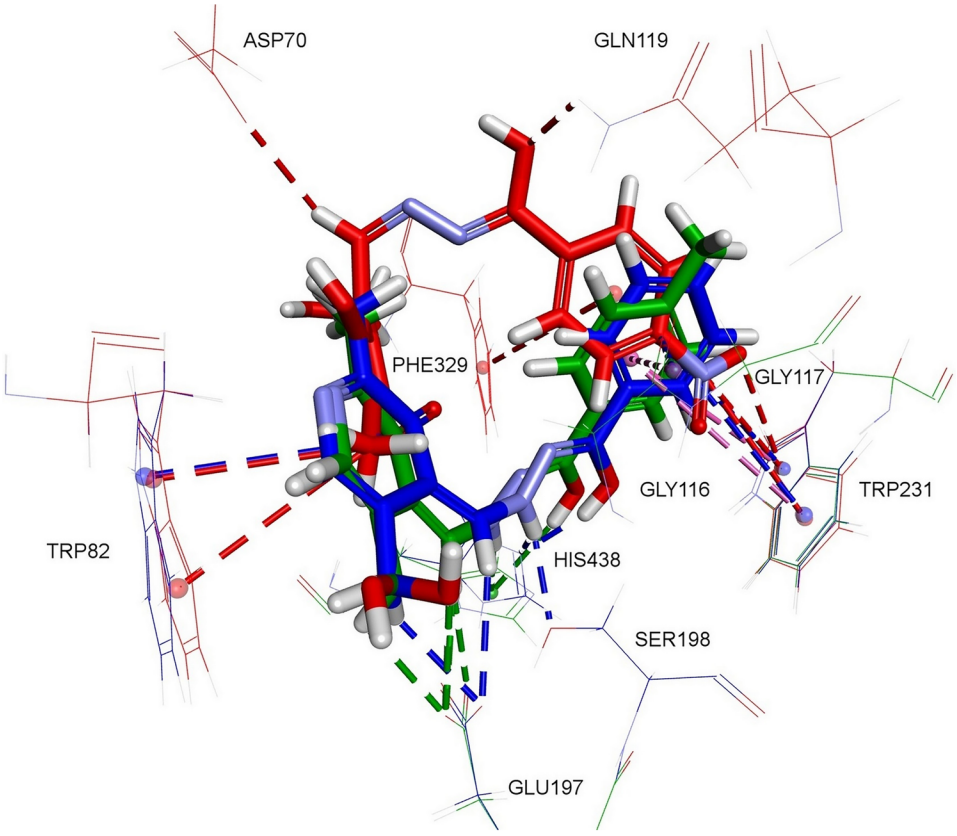

Figure 3. Complex of BChE and **9** (carbon atoms and interactions in blue), **10** (carbon atoms and interactions in red) and **13** (carbon atoms and interactions in green).

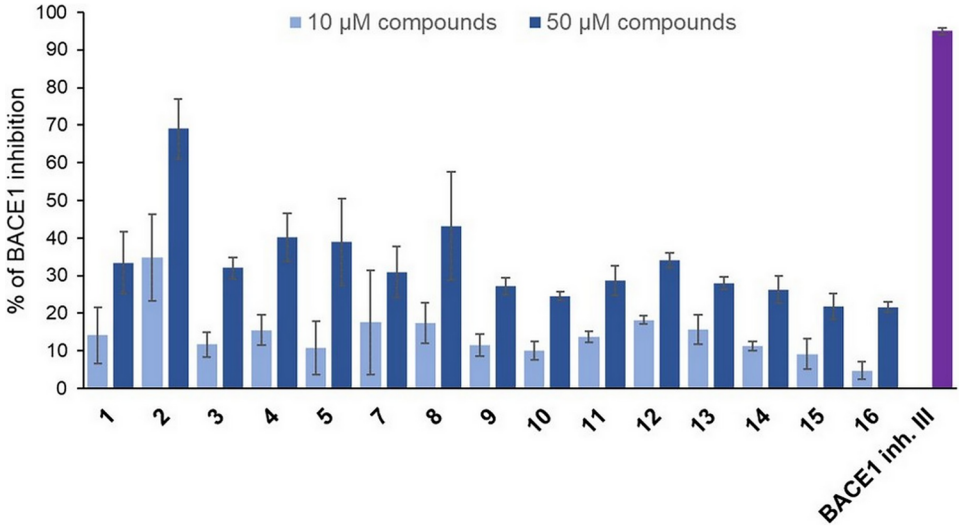

Figure 4. Inhibition of BACE1 activity.

incubation period (Figure 7(A)) were chosen for differential spectra analysis (Figure 7(B)), as after 30 min the spectra of the hydrazone–metal mixture did not change. Differential spectra confirmed the chelating ability of hydrazone (Figures S37–S39).

For all of the hydrazone and biometal mixtures, changes in the spectra-like shifts of peaks in absorption spectra or intensity of absorption of hydrazone–metal mixtures compared to the spectra of hydrazones were observed, which is evidence of the formation of a metal–hydrazone complex[51].

ADME properties

Ability to cross the BBB

The ability of all of the tested hydrazones to cross the BBB by passive transport was estimated by comparing the calculated values of six physicochemical descriptors of compounds (Table S36) with recommended values obtained for known central nervous system (CNS)-active drugs[57,70–72]. CNS-active drugs generally have a molecular weight lower than 500 g mol^{-1}, moderate hydrophobicity (logP < 5), less than five hydrogen bonds donors (HBD), less

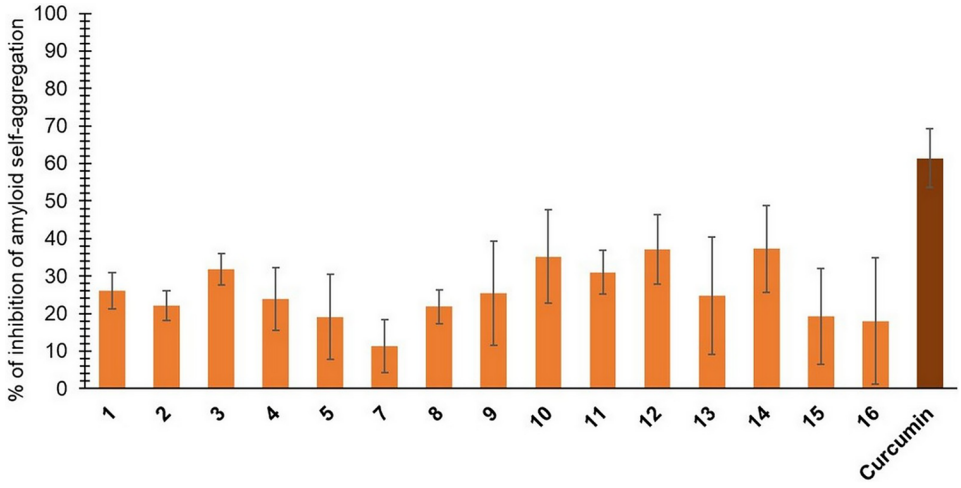

Figure 5. Inhibition of Aβ42 self-aggregation.

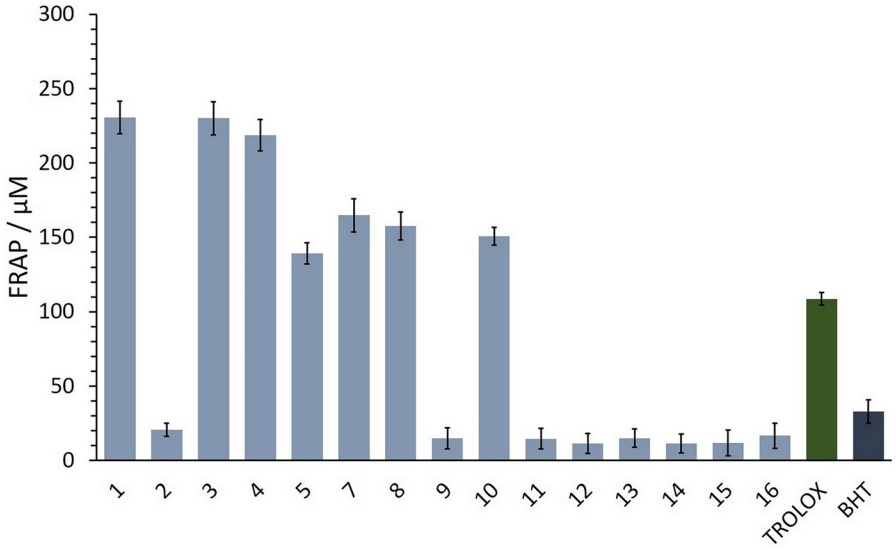

Figure 6. The FRAP values. Columns denote FRAP values for a 50 μM compound.

than five hydrogen bond acceptors (HBA), and less than ten rotatable bonds (RB) and are less polar (polar surface area (PSA) < 90 Å2) than drugs that are not active in the CNS. For six hydrazones (**1**, **3**, **4**, **5**, **7** and **8**), the *in silico* determined physicochemical descriptors were in the range of the upper recommended values (Figure 8), based on which it was estimated that they should be able to pass the BBB. Although hydrazones **9** and **11** have a larger PSA compared to the recommended value, it can be expected that these compounds would be able to pass the BBB since according to the literature, compounds that violate only one of the six physicochemical properties, could cross the BBB[57,72]. Compounds **2, 10** and **13**–**16** had two descriptors outside of the recommended value and it is not likely that they would cross the BBB by passive transport.

Evaluation of human intestine absorption

The percentage of hydrazones that would be absorbed through the human intestine was estimated *in silico* using the pkCSM prediction model. According to the model, with the absorption percentage in the range between 72 and 93 (Table S37), all of the compounds would likely be very well-absorbed in the human intestines.

Metabolic stability

To determine whether and how fast the compound of interest is metabolised, a metabolic stability of compounds **1**, **2**, **4**, **5**, **8** and **12,** selected based on their high ability to inhibit the action of AChE, BChE, and BACE1, was determined *in vitro* in human liver microsomes (Table 3). According to the values of LBF clearance, the selected hydrazones are moderate or high metabolic stable compounds, which indicates their good bioavailability.

Inhibition of cytochrome P450 enzymes

Since microsomal CYP450 enzymes catalyse oxidative biotransformation of xenobiotics to facilitate their excretion, inhibition of P450 leads to toxic or other unwanted adverse effects. *In silico* prediction of P450 sub-types (CYP1A2, CYP2C19, CYP2C9, CYP2D6 and CYP3A4) inhibition (Table S36) showed that majority of compounds do not inhibit CYP enzymes. The exception was CYP1A2, which was estimated to be inhibited by as many as seven out of a total of 16 tested compounds.

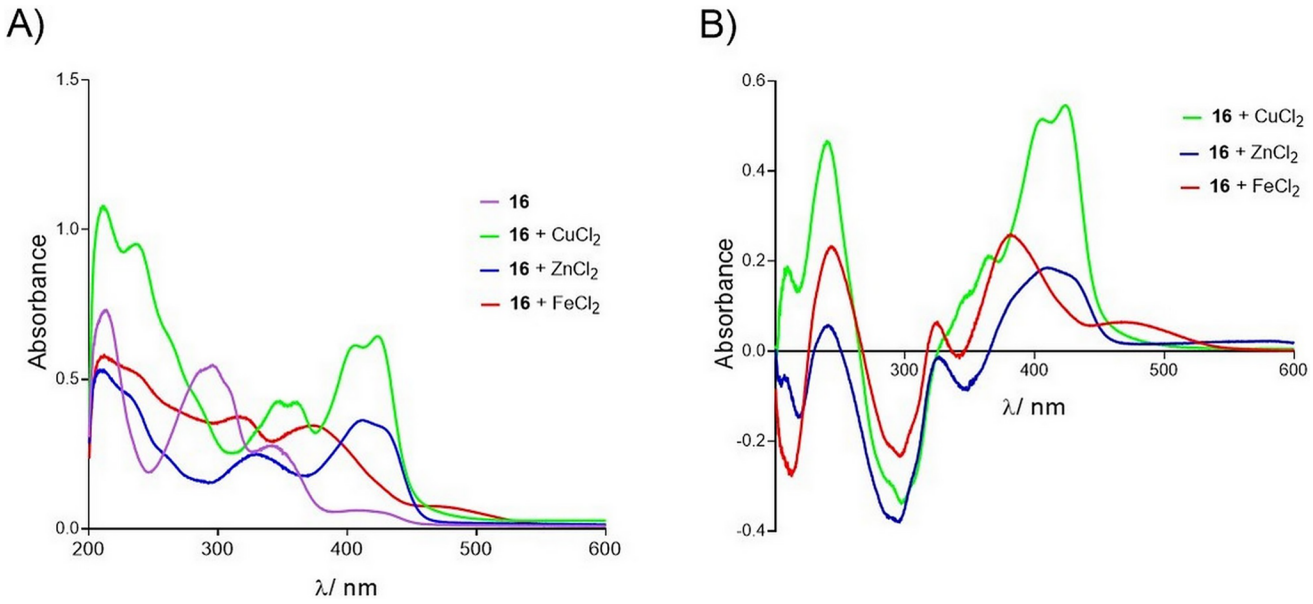

Figure 7. UV–VIS spectra of **2** (purple) and after mixing with Cu^{2+} (green), Zn^{2+} (blue) and Fe^{2+} (red) (panel A). The differential spectra of **2**-Cu^{2+} (green), **2**-Zn^{2+} (blue) and **2**-Fe^{2+} complexes (red) (panel B).

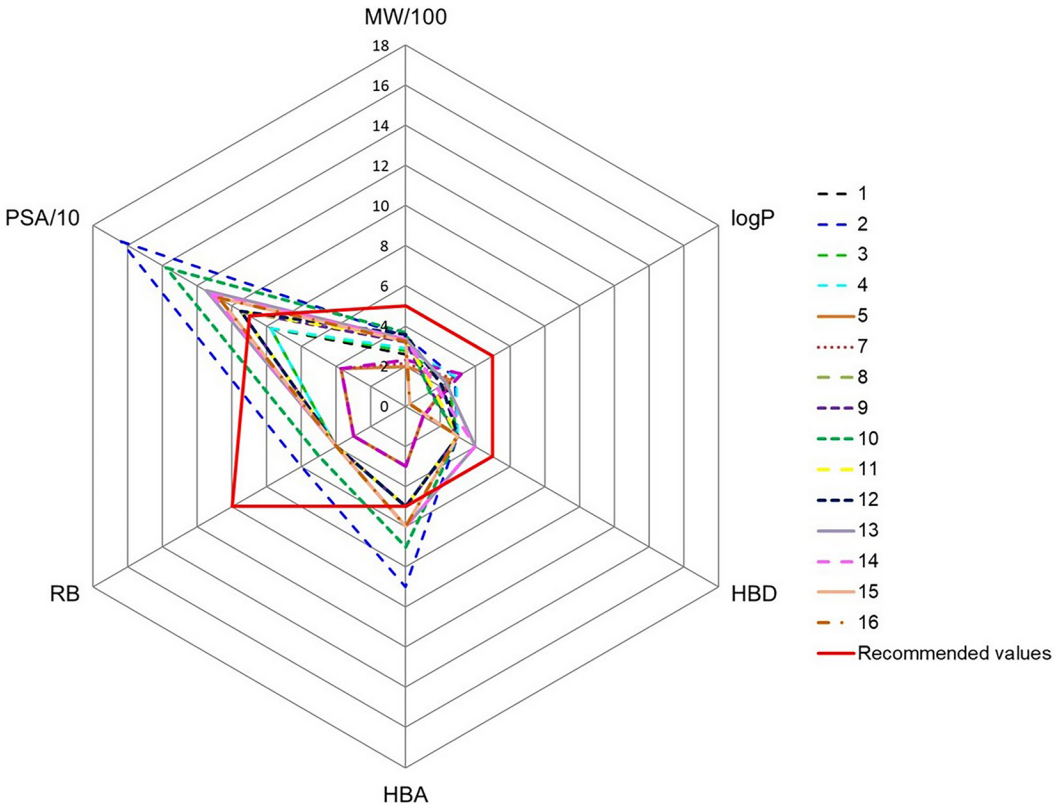

Figure 8. Radar plot of physicochemical properties (molecular weight (MW), lipophilicity coefficient (logP), number of hydrogen bonds donors (HBD) and acceptors (HBA), number of rotatable bonds (RB), polar surface area (PSA) of the tested hydrazones. The recommended values for the CNS-active drugs are presented by a red line.

Conclusion

We have shown that hydrazone derivatives of vitamin B6 and pyridine-4-carbaldehyde are very promising molecules for the development of multi-target AD drugs targeting AChE and BChE, the enzymes involved in maintaining acetylcholine levels in the brain as a prerequisite action for the symptomatic treatment of AD, and simultaneously acting against the mechanisms involved in onset and progression of the disease by inhibition of BACE1, one of the regulatory enzymes involved in the accumulation of β-amyloid plaques, and inhibition of self-aggregation of β-amyloid fibrils itself. The additional beneficial action of our hydrazone

Table 3. Metabolic stability of the selected hydrazones.

Compound	%LBF	Metabolic stability
1	63	moderate
2	43	moderate
4	<30	high
5	39	moderate
8	<30	high
12	57	moderate

derivatives is their ability to provide an effective defence against oxidative stress and maintain the redox balance by chelating metal ions Fe(II), Cu(II) and Zn(II), and through their significant antioxidant power equally or even more potent as that of standard antioxidants. All of the compounds possessed at least four favourable activities against different causative mechanisms which they exerted in comparable concentration ranges. In addition, most of the compounds displayed a type of reversible inhibition that included interactions with AChE PAS suggesting that those compounds could be able to prevent the formation of neurotoxic AChE–Aß complexes. This study singled out two compounds as the most promising multi-target drugs differing in selectivity towards cholinesterases: **1** as butyrylcholinesterase-selective and **4** as a non-selective cholinesterase inhibitor, but all with high inhibition potency towards BACE1, ability to inhibit amyloid-β self-aggregation, to chelate all three metal cations and high ability to act as antioxidants. An *in vitro* assessment of the possibility of passing through the blood–brain barrier and good intestinal permeability also spoke in support of this. Additionally, the metabolic stability of those compounds should allow them to achieve and maintain sufficient concentrations at their sites of action and to be slowly removed from the body. The fact that these compounds can be successfully synthesised in conventional and environmentally friendly ways highlights them, especially given their structural scaffold, as good models for structural and functional refinement in terms of multi-target drug development.

Acknowledgements

The authors are grateful to Dr Florian Nachon (Département de Toxicologie, Armed Forces Biomedical Research Institute, France) for providing us with the AChE and BChE, and to Makso Herman for proofreading the paper. This study was performed using the facilities and equipment funded within ERDF project KK.01.1.1.02.0007 ReC-IMI.

Disclosure statement

The authors declare no conflict of interest and no competing financial interest.

Funding

The work was supported by the CSF (Grant No. HrZZ-IP-2020–02-9343).

Data availability statement

The data presented in this study are available on request from the corresponding author.

References

1. Silva MVF, Loures CMG, Alves LCV, Souza LC, Borges KBG, Carvalho MG. Alzheimer's disease: risk factors and potentially protective measures. J Biomed Sci. 2019;26(1):33.
2. Zvěřová M. Clinical aspects of Alzheimer's disease. Clin Biochem. 2019;72:3–6.
3. Koelsch G. BACE1 function and inhibition: implications of intervention in the amyloid pathway of Alzheimer's disease pathology. Molecules. 2017;22(10):1723.
4. Francis PT, Palmer AM, Snape M, Wilcock GK. The cholinergic hypothesis of Alzheimer's disease: a review of progress. J Neurol Neurosurg Psychiatry. 1999;66(2):137–147.
5. Abeysinghe ADT, Deshapriya RDUS, Udawatte C. Alzheimer's disease: a review of the pathophysiological basis and therapeutic interventions. Life Sci. 2020;256:e117996.
6. Söderberg L, Johannesson M, Nygren P, Laudon H, Eriksson F, Osswald G, Möller C, Lannfelt L. Lecanemab, aducanumab, and gantenerumab – binding profiles to different forms of amyloid-beta might explain efficacy and side effects in clinical trials for Alzheimer's disease. Neurotherapeutics. 2023;20(1):195–206.
7. Mahase E. Aducanumab: European agency rejects Alzheimer's drug over efficacy and safety concerns. BMJ. 2021;375:n3127.
8. Kinney JW, Bemiller SM, Murtishaw AS, Leisgang AM, Salazar AM, Lamb BT. Inflammation as a central mechanism in Alzheimer's disease. Alzheimers Dement (NY). 2018;4(1):575–590.
9. Li Y, Jiao Q, Xu H, Du X, Shi L, Jia F, Jiang H. Biometal dyshomeostasis and toxic metal accumulations in the development of Alzheimer's disease. Front Mol Neurosci. 2017;10:339.
10. Huang WJ, Zhang X, Chen WW. Role of oxidative stress in Alzheimer's disease (review). Biomed Rep. 2016;4(5):519–522.
11. Zhou J, Jiang X, He S, Jiang H, Feng F, Liu W, Qu W, Sun H. Rational design of multi-target-directed ligands: strategies and emerging paradigms. J Med Chem. 2019;62(20):8881–8914.
12. Iraji A, Khoshneviszadeh M, Firuzi O, Khoshneviszadeh M, Edraki N. Novel small molecule therapeutic agents for Alzheimer disease: focusing on BACE1 and multi-target directed ligands. Bioorg Chem. 2020;97:103649.
13. Sang Z, Wang K, Shi J, Liu W, Cheng X, Zhu G, Wang Y, Zhao Y, Qiao Z, Wu A, et al. The development of advanced structural framework as multi-target directed ligands for the treatment of Alzheimer's disease. Eur J Med Chem. 2020;192:112180.
14. Hafez DE, Dubiel M, La Spada G, Catto M, Reiner-Link D, Syu Y-T, Abdel-Halim M, Hwang T-L, Stark H, Abadi AH. Novel benzothiazole derivatives as multitargeted-directed ligands for the treatment of Alzheimer's disease. J Enzyme Inhib Med Chem. 2023;38(1):2175821.
15. Mesiti F, Chavarria D, Gaspar A, Alcaro S, Borges F. The chemistry toolbox of multitarget-directed ligands for Alzheimer's disease. Eur J Med Chem. 2019;181:111572.
16. Rollas S, Küçükgüzel ŞG. Biological activities of hydrazone derivatives. Molecules. 2007;12(8):1910–1939.
17. Silva Mde F, Lima ET, Pruccoli L, Castro NG, Guimarães MJR, da Silva FMR, Nadur NF, de Azevedo LL, Kümmerle AE, Guedes IA, et al. Design, synthesis and biological evaluation of novel triazole *N*-acylhydrazone hybrids for Alzheimer's disease. Molecules. 2020;25(14):e3165.
18. Petronilho EdC, Rennó MdN, Castro NG, da Silva FMR, Pinto AdC, Figueroa-Villar JD. Design, synthesis, and evaluation of guanylhydrazones as potential inhibitors or reactivators of

acetylcholinesterase. J Enzyme Inhib Med Chem. 2016;31(6):1069–1078.
19. Krátký M, Štěpánková Š, Konečná K, Svrčková K, Maixnerová J, Švarcová M, Janďourek O, Trejtnar F, Vinšová J. Novel aminoguanidine hydrazone analogues: from potential antimicrobial agents to potent cholinesterase inhibitors. Pharmaceuticals. 2021;14(12):e1229.
20. Prinz M, Parlar S, Bayraktar G, Alptüzün V, Erciyas E, Fallarero A, Karlsson D, Vuorel P, Burek M, Förster C, et al. 1,4-Substituted 4-(1H)-pyridylene-hydrazone-type inhibitors of AChE, BuChE, and amyloid-b aggregation crossing the blood–brain barrier. Eur J Pharm Sci. 2013;49(4):603–613.
21. Cukierman DS, Accardo E, Gomes RG, De Falco A, Miotto MC, Ramalho Freitas MC, Lanznaster M, Fernández CO, Rey NA. Aroylhydrazones constitute a promising class of 'metal–protein attenuating compounds' for the treatment of Alzheimer's disease: a proof-of-concept based on the study of the interactions between zinc(II) and pyridine-2-carboxaldehyde isonicotinoyl hydrazone. J Biol Inorg Chem. 2018;23(8):1227–1241.
22. Hauser-Davis RA, de Freitas LV, Cukierman DS, Cruz WS, Miotto MC, Landeira-Fernandez J, Valiente-Gabioud AA, Fernándezb CO, Rey NA. Disruption of zinc and copper interactions with Ab(1–40) by a non-toxic, isoniazid-derived hydrazone: a novel biometal homeostasis restoring agent in Alzheimer's disease therapy? Metallomics. 2015;7(5):743–747.
23. McInnes LE, Noor A, Roselt PD, McLean CA, White JM, Donnelly PS. A copper complex of a thiosemicarbazone-pyridylhydrazone ligand containing a vinylpyridine functional group as a potential imaging agent for amyloid-β plaques. Aust J Chem. 2019;72(10):827–830.
24. Parra M, Stahl S, Hellmann H. Vitamin B_6 and its role in cell metabolism and physiology. Cells. 2018;7(7):e84.
25. Shtyrlin YG, Petukhov AS, Strelnik AD, Shtyrlin NV, Iksanova AG, Pugachev MV, Pavelyev RS, Dzyurkevich MS, Garipov MR, Balakin KV. Chemistry of pyridoxine in drug design. Russ Chem Bull. 2019;68(5):911–945.
26. Chen X, Li H, Luo H, Lin Z, Luo W. Synthesis and evaluation of pyridoxal hydrazone and acylhydrazone compounds as potential angiogenesis inhibitors. Pharmacology. 2019;104(5–6):244–257.
27. Nogueira TCM, dos Santos Cruz L, Lourenço MC, de Souza MVN. Design, synthesis and anti-tuberculosis activity of hydrazones and *N*-acylhydrazones containing vitamin B6 and different heteroaromatic nucleus. LDDD. 2019;16(7):792–798.
28. Vlad IM, Nuță DC, Căproiu MT, Dumitrașcu F, Kapronczai E, Mük GR, Avram S, Niculescu AG, Zarafu I, Ciorobescu VA, et al. Synthesis and characterization of new *N*-acyl hydrazone derivatives of carprofen as potential tuberculostatic agents. Antibiotics (Basel). 2024;13(3):212.
29. Buss JL, Hermes-Lima M, Ponka P. Pyridoxal isonicotinoyl hydrazone and its analogues. Adv Exp Med Biol. 2002;509:205–229.
30. GBD 2019 Dementia Forecasting Collaborators . Estimation of the global prevalence of dementia in 2019 and forecasted prevalence in 2050: an analysis for the global burden of disease study 2019. Lancet Public Health. 2022;7(2):105–125.
31. Gangrade D, Lad SD, Mehta AL. Overview on microwave synthesis – important tool for green chemistry. Int J Res Pharm Sci. 2015;5(2):37–42.
32. Berrino E, Supuran CT. Advances in microwave-assisted synthesis and the impact of novel drug discovery. Expert Opin Drug Discov. 2018;13(9):861–873.
33. Dudley GB, Stiegman AE. Changing perspectives on the strategic use of microwave heating in organic synthesis. Chem Rec. 2018;18(3):381–389.
34. Bušić V, Vrandečić K, Siber T, Roca S, Tomičić V, Gašo- Sokač D. Novel synthetic routes to quaternary pyridinium salts and their antifungal activity. Croat Chem Acta. 2022;95(1):31–38.
35. Sharma S, Dubey G, Singh Sran B, Sharma M, Kaur V, Kaur S, Bharatam PV, Hundal G. Hundal Microwave-induced synthesis of pyridine based Schiff bases and their applications as efficient antimicrobial textile dyeing agents: experimental and theoretical approach. Chem Select. 2022;7(45):e202203109.
36. Kennedy ME, Stamford AW, Chen X, Cox K, Cumming JN, Dockendorf MF, Egan M, Ereshefsky L, Hodgson RA, Hyde LA, et al. The BACE1 inhibitor verubecestat (MK-8931) reduces CNS β-amyloid in animal models and in Alzheimer's disease patients. Sci Transl Med. 2016;8(363):363ra150.
37. Egan MF, Mukai Y, Voss T, Kost J, Stone J, Furtek C, Mahoney E, Cummings JL, Tariot PN, Aisen PS, et al. Further analyses of the safety of verubecestat in the phase 3 EPOCH trial of mild-to-moderate Alzheimers disease. Alzheimers Res Ther. 2019;11(1):68. article no
38. Timmers M, Streffer JR, Russu A, Tominaga Y, Shimizu H, Shiraishi A, Tatikola K, Smekens P, Börjesson-Hanson A, Andreasen N, et al. Pharmacodynamics of atabecestat (JNJ-54861911), an oral BACE1 inhibitor in patients with early Alzheimer's disease: randomized, double-blind, placebo-controlled study. Alzheimers Res Ther. 2018;10(1):85.
39. Novak G, Streffer JR, Timmers M, Henley D, Brashear HR, Bogert J, Russu A, Janssens L, Tesseur I, Tritsmans L, et al. Long-term safety and tolerability of atabecestat (JNJ-54861911), an oral BACE1 inhibitor, in early Alzheimer's disease spectrum patients: a randomized, double-blind, placebo-controlled study and a two-period extension study. Alzheimers Res Ther. 2020;12(1):58.
40. Ellman GL, Courtney KD, Andres VJr, Feather-Stone RM. A new and rapid colorimetric determination of acetylcholinesterase activity. Biochem Pharmacol. 1961;7(2):88–95.
41. Simeon-Rudolf V, Šinko G, Štuglin A, Reiner E. Inhibition of human blood acetylcholinesterase and butyrylcholinesterase by ethopropazine. Croat Chem Acta. 2001;74(1):173–182.
42. β-Secretase (BACE1) Activity Detection Kit (Fluorescent) – https://www.sigmaaldrich.com/HR/en/product/sigma/cs0010?srsltid=AfmBOop7Ksh9XRoWEcWPpWJuixSftt_8xzIlwC9W5_G1-Fyd5igyfCpr.
43. Matošević A, Opsenica D, Spasić M, Maraković N, Zandona A, Žunec S, Bartolić M, Kovarik Z, Bosak A. Evaluation of 4-aminoquinoline derivatives with an *n*-octylamino spacer as potential multi-targeting ligands for the treatment of Alzheimer's disease. Chem Biol Interact. 2023;382:110620.
44. β-Secretase inhibitor III – calbiochem. https://www.merckmillipore.com/INTL/en/product/-Secretase-Inhibitor-III-Calbiochem,EMD_BIO-565780? ReferrerURL=https%3A%2F%2Fwww.google.com/.
45. Xue C, Lin TY, Chang D, Guo Z. Thioflavin T as an amyloid dye: fibril quantification, optimal concentration and effect on aggregation. R Soc Open Sci. 2017;4(1):160696.
46. Stefanescu R, Stanciu GD, Luca A, Paduraru L, Tamba B-I. Secondary metabolites from plants possessing inhibitory properties against beta-amyloid aggregation as revealed by thioflavin-T assay and correlations with investigations on transgenic mouse models of Alzheimer's disease. Biomolecules. 2020;10(6):870.
47. Török B, Sood A, Bag S, Tulsan R, Ghosh S, Borkin D, Kennedy AR, Melanson M, Madden R, Zhou W, et al. Diaryl hydrazones

as multifunctional inhibitors of amyloid self-assembly. Biochemistry. 2013;52(7):1137–1148.
48. Sagnou M, Mavroidi B, Kaminari A, Boukos N, Pelecanou M. Novel isatin thiosemicarbazone derivatives as potent inhibitors of β-amyloid peptide aggregation and toxicity. ACS Chem Neurosci. 2020;11(15):2266–2276.
49. Yang F, Lim GP, Begum AN, Ubeda OJ, Simmons MR, Ambegaokar SS, Chen PP, Kayed R, Glabe CG, Frautschy SA, et al. Curcumin inhibits formation of amyloid β oligomers and fibrils, binds plaques, and reduces amyloid *in vivo*. J Biol Chem. 2005;280(7):5892–5901.
50. Matošević A, Knežević A, Zandona A, Maraković N, Kovarik Z, Bosak A. Design, synthesis and biological evaluation of bis-carbamates as potential selective butyrylcholinesterase inhibitors for the treatment of Alzheimer's disease. Pharmaceuticals. 2022;15(10):1220.
51. Bolognesi ML, Cavalli A, Valgimigli L, Bartolini M, Rosini M, Andrisano V, Recanatini M, Melchiorre C. Multi-target-directed drug design strategy: from a dual binding site acetylcholinesterase inhibitor to a trifunctional compound against Alzheimer's disease. J Med Chem. 2007;50(26):6446–6449.
52. Benzie IF, Strain JJ. Ferric reducing/antioxidant power assay: direct measure of total antioxidant activity of biological fluids and modified version for simultaneous measurement of total antioxidant power and ascorbic acid concentration. Methods Enzymol. 1999;299:15–27.
53. Jalili-Baleh L, Nadri H, Forootanfar H, Küçükkılınç TT, Ayazgök B, Sharifzadeh M, Rahimifard M, Baeeri M, Abdollahi M, Foroumadi A, et al. Chromone–lipoic acid conjugate: neuroprotective agent having acceptable butyrylcholinesterase inhibition, antioxidant and copper-chelation activities. Daru. 2021;29(1):23–38.
54. Cheung J, Rudolph MJ, Burshteyn F, Cassidy MS, Gary EN, Love J, Franklin MC, Height JJ. Structures of human acetylcholinesterase in complex with pharmacologically important ligands. J Med Chem. 2012;55(22):10282–10286.
55. Nicolet Y, Lockridge O, Masson P, Fontecilla-Camps JC, Nachon F. Crystal structure of human butyrylcholinesterase and of its complexes with substrate and products. J Biol Chem. 2003;278(42):41141–41147.
56. Komatović K, Matošević A, Terzić-Jovanović N, Žunec S, Šegan S, Zlatović M, Maraković N, Bosak A, Opsenica DM. 4-aminoquinoline-based adamantanes as potential anticholinesterase agents in symptomatic treatment of Alzheimer's disease. Pharmaceutics. 2022;14(6):1305.
57. Chemicalize, Calculation Module 2, 2018 https://chemicalize.com/developed. by ChemAxon http://www.chemaxon.com.
58. Pajouhesh H, Lenz GR. Medicinal chemical properties of successful central nervous system drugs. NeuroRx. 2005;2(4):541–553.
59. Pires DEV, Blundell TL, Ascher DB. pkCSM: predicting small-molecule pharmacokinetic and toxicity properties using graph-based signatures. J Med Chem. 2015;58(9):4066–4072.
60. Słoczyńska K, Gunia-Krzyżak A, Koczurkiewicz P, Wójcik-Pszczoła K, Żelaszczyk D, Popiół J, Pękala E. Metabolic stability and its role in the discovery of new chemical entities. Acta Pharm. 2019;69(3):345–361.
61. https://biosig.lab.uq.edu.au/pkcsm/theory. (accessed on 2024 Oct 22)
62. Bušić V, Roca S, Gašo-Sokač D. Application of choline chloride-based deep eutectic solvents in the synthesis of hydrazones. Separations. 2023;10(11):551.
63. Darvesh S, Walsh R, Kumar R, Caines A, Roberts S, Magee D, Rockwood K, Martin E. Inhibition of human cholinesterases by drugs used to treat Alzheimer disease. Alzheimer Dis Assoc Disord. 2003;17(2):117–126.
64. Younas MT, Zaib S, Khan I. Discovery of hydrazone scaffolds as potent and selective multitarget-directed ligands for the treatment of neurodegenerative disorders. Chem Select. 2023;8(47):e202303089.
65. Choubey PK, Tripathi A, Tripathi MK, Seth A, Shrivastava SK. Design, synthesis, and evaluation of *N*-benzylpyrrolidine and 1, 3, 4-oxadiazole as multitargeted hybrids for the treatment of Alzheimer's disease. Bioorg Chem. 2021;111:104922.
66. Sinha SK, Shrivastava SK. Synthesis, evaluation and molecular dynamics study of some new 4-aminopyridine semicarbazones as an antiamnesic and cognition enhancing agents. Bioorg Med Chem. 2013;21(17):5451–5460.
67. Greig NH, Lahiri DK, Sambamurti K. Butyrylcholinesterase: an important new target in Alzheimer's disease therapy. Int Psychogeritar. 2002;14(1):77–91.
68. McDade E, Voytyuk I, Aisen P, Bateman RJ, Carrillo MC, De Strooper B, Haass C, Reiman EM, Sperling R, Tariot PN, et al. The case for low-level BACE1 inhibition for the prevention of Alzheimer's disease. Nat Rev Neurol. 2021;17(11):703–714.
69. Maloney A, Bainbridge T, Gustafson A, Zhang S, Kyauk R, Steiner P, van der Brug M, Liu Y, Ernst JA, Watts RJ, et al. Molecular mechanisms of Alzheimer disease protection by the A673T allele of amyloid precursor protein. J Biol Chem. 2014;289(45):30990–31000.
70. Pal T, Patil P, Shrama A. Synthesis, *in silico*, molecular docking and spectroscopic studies of pyridoxine carbamates as metal chelator. J Mol Struct. 2021;1223:1–13.
71. Lipinski CA, Lombardo F, Dominy BW, Feeney PJ. Experimental and computational approaches to estimate solubility and permeability in drug discovery and development settings. Adv Drug Deliv Rev. 2001;46(1–3):3–26.
72. Veber DF, Johnson SR, Cheng HY, Smith BR, Ward KWI, Kopple KD. Molecular properties that influence the oral bioavailability of drug candidates. J Med Chem. 2002;45(12):2615–2623.